

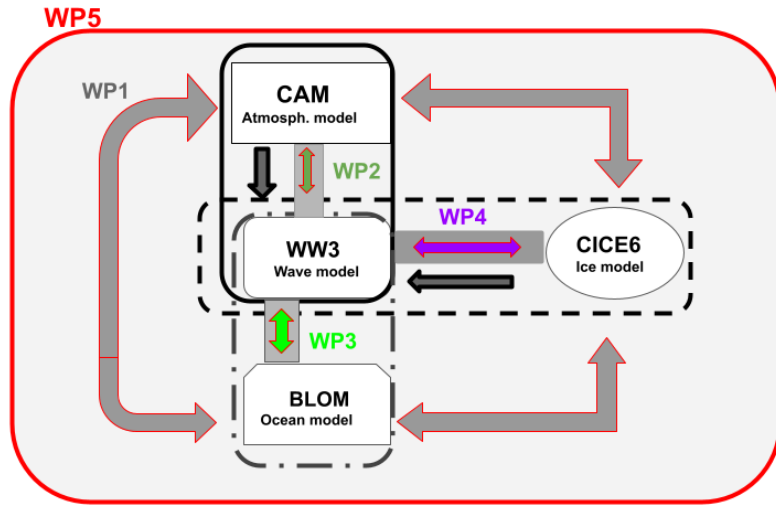
Effects of
atmosphere-surface ocean waves
two-way coupling
on the simulated climatology
of the North
Atlantic

Thomas Toniazzo (NORCE and Bjerknes Centre, Bergen, Norway)

Fifth workshop on waves and wave-coupled Processes
ECMWF, Reading, 10 April 2024

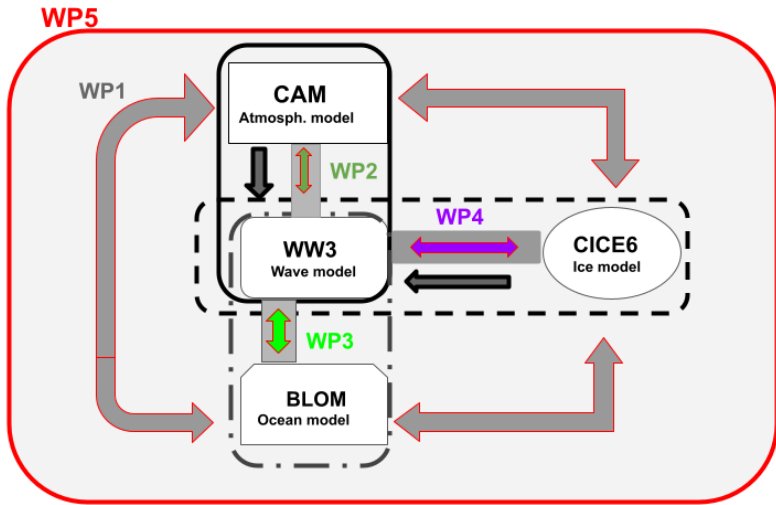
The “Making Waves” collaboration

*Ana Carrasco, Ali Alfatih, Mats Bentsen, Øyvind Breivik, Kai Christensen,
Jens Debernard, Thea Ellevold, Alexi Nummelin, Thomas Toniazzo
(ackn. Mariana Vertenstein)*



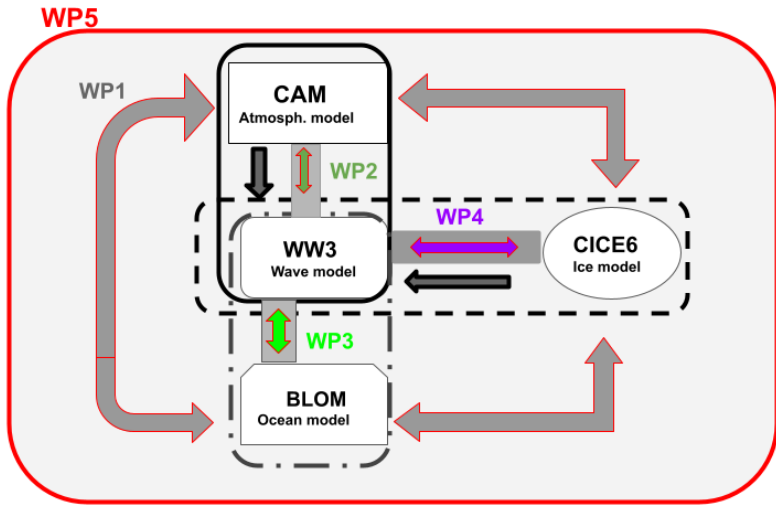
- Drawing from different experience in
 - Operational forecasting
 - Climate simulations
- Combining existing expertise on waves, ocean, sea-ice, and atmosphere
- Include wave effects in climate simulations
 - Air-sea fluxes
 - Ocean mixing and mechanical forcing
 - Sea-ice growth and break-up

Ocean waves and climate



- Operational use of surface wave models mature in weather forecasting
- Main documented effect is the enhanced barometric filling of strong depressions due to increased surface friction
- climate simulations aimed to understand **potential** effects associated with
 - Persistent changes in distribution of air-sea fluxes and diabatic heating of atmosphere
 - Ocean stirring and mixed-layer deepening
 - WRS on and break-up of marginal ice
- Coupling might amplify individual effects

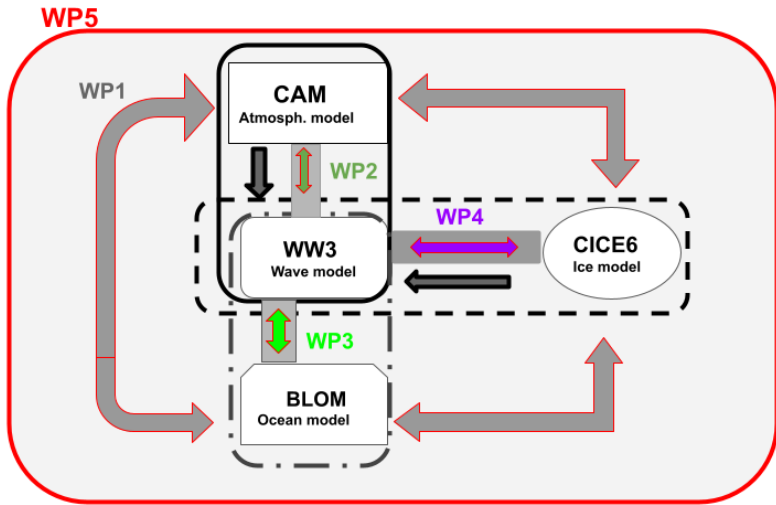
Ocean waves and climate



- Operational use of surface wave models mature in weather forecasting
- Main documented effect is the enhanced barometric filling of strong depressions due to increased surface friction
- climate simulations aimed to understand *potential* effects associated with
 - Persistent changes in distribution of air-sea fluxes and diabatic heating of atmosphere
 - Ocean stirring and mixed-layer deepening
 - WRS on and break-up of marginal ice
- Coupling might amplify individual effects

This talk

Ocean waves and climate



- Operational use of surface wave models mature in weather forecasting
- Main documented effect is the enhanced barometric filling of strong depressions due to increased surface friction
- climate simulations aimed to understand **potential** effects associated with
 - Persistent changes in distribution of air-sea fluxes and diabatic heating of atmosphere
 - Ocean stirring and mixed-layer deepening
 - WRS on and break-up of marginal ice
- Coupling might amplify individual effects

Also in this workshop:

Øyvind Breivik (MET Norway), Thu 9am

Alfatih Ali (MET Norway), poster

COARE 3 (Fairall et al. 2013) + Drennan et al. (2005)

$$\left\{ \begin{array}{l} u_*^2 = C_D [U(z) - U_s]^2 \\ C_D = \frac{\kappa^2}{[\Psi(z + z_0) - \Psi(z_0)]^2} \\ z_0 = a \frac{u_*^2}{g} + b \frac{v}{u_*} \end{array} \right.$$

COARE 3 (Fairall et al. 2013) + Drennan et al. (2005)

$$\left\{ \begin{array}{l} u_*^2 = C_D [U(z) - U_s]^2 \\ C_D = \frac{\kappa^2}{[\Psi(z + z_0) - \Psi(z_0)]^2} \\ z_0 = a \frac{u_*^2}{g} + b \frac{\nu}{u_*} \end{array} \right.$$

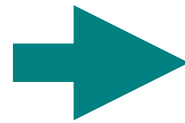
“Charnock parameter”



QL theory of Janssen (1989, 1991); Varlas et al. (2018)

$$\left\{ \begin{array}{l} u_*^2 = C_D [U(z) - U_s]^2 \\ C_D = \frac{K^2}{[\Psi(z+z_0) - \Psi(z_0)]^2} \\ z_0 = a \frac{u_*^2}{g} + b \frac{v}{u_*} \end{array} \right.$$

“Charnock parameter”

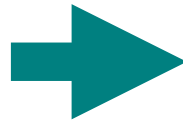


“wave Charnock parameter”

$$\left\{ \begin{array}{l} u_*^2 = C_D [U(z) - U_s]^2 \\ C_D = \frac{K^2}{[\Psi(z+z_0) - \Psi(z_0)]^2} \\ z_0 = a \frac{u_*^2}{g} + b \frac{v}{u_*} \\ a = \hat{a} [1 - u_w^2 / u_*^2]^{-1/2} \\ u_w^2 = g \int d\omega d\theta \gamma' N k \\ \gamma' = \gamma'(z_0, u_*) \end{array} \right.$$

QL theory of Janssen (1989, 1991); Varlas et al. (2018)

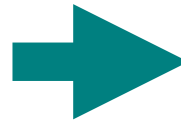
$$\left\{ \begin{aligned} u_*^2 &= C_D [U(z) - U_s]^2 \\ C_D &= \frac{K^2}{[\Psi(z+z_0) - \Psi(z_0)]^2} \\ z_0 &= a \frac{u_*^2}{g} + b \frac{v}{u_*} \end{aligned} \right.$$



$$\left\{ \begin{aligned} u_*^2 &= C_D [U(z) - U_s]^2 \\ C_D &= \frac{K^2}{[\Psi(z+z_0) - \Psi(z_0)]^2} \\ z_0 &= a \frac{u_*^2}{g} + b \frac{v}{u_*} \\ a &= \hat{a} [1 - u_w^2 / u_*^2]^{-1/2} \\ u_w^2 &= g \int d\omega d\theta \gamma' N k \\ \gamma' &= \gamma'(z_0, u_*) \end{aligned} \right.$$

QL theory of Janssen (1989, 1991); Varlas et al. (2018)

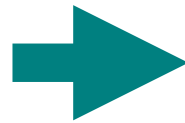
$$\left\{ \begin{aligned} u_*^2 &= C_D [U(z) - U_s]^2 \\ C_D &= \frac{K^2}{[\Psi(z+z_0) - \Psi(z_0)]^2} \\ z_0 &= a \frac{u_*^2}{g} + b \frac{v}{u_*} \end{aligned} \right.$$



$$\left\{ \begin{aligned} u_*^2 &= C_D [U(z) - U_s]^2 \\ C_D &= \frac{K^2}{[\Psi(z+z_0) - \Psi(z_0)]^2} \\ z_0 &= a \frac{u_*^2}{g} + b \frac{v}{u_*} \\ a &= \hat{a} [1 - u_w^2 / u_*^2]^{-1/2} \\ u_w^2 &= g \int d\omega d\theta \gamma' N k \\ \gamma' &= \gamma'(z_0, u_*) \end{aligned} \right.$$

QL theory of Janssen (1989, 1991); Varlas et al. (2018)

$$\left\{ \begin{aligned} u_*^2 &= C_D [U(z) - U_s]^2 \\ C_D &= \frac{K^2}{[\Psi(z+z_0) - \Psi(z_0)]^2} \\ z_0 &= a \frac{u_*^2}{g} + b \frac{v}{u_*} \end{aligned} \right.$$



$$\left\{ \begin{aligned} u_*^2 &= C_D [U(z) - U_s]^2 \\ C_D &= \frac{K^2}{[\Psi(z+z_0) - \Psi(z_0)]^2} \\ z_0 &= a \frac{u_*^2}{g} + b \frac{v}{u_*} \\ a &= \hat{a} [1 - u_w^2 / u_*^2]^{-1/2} \\ u_w^2 &= g \int d\omega d\theta \gamma' N k \\ \gamma' &= \gamma'(z_0, u_*) \end{aligned} \right.$$

QL theory of Janssen (1989, 1991); Varlas et al. (2018)

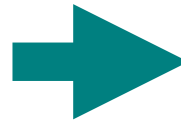
$$\left\{ \begin{aligned} u_*^2 &= C_D [U(z) - U_s]^2 \\ C_D &= \frac{\kappa^2}{[\Psi(z+z_0) - \Psi(z_0)]^2} \\ z_0 &= a \frac{u_*^2}{g} + b \frac{\nu}{u_*} \end{aligned} \right.$$

$$\int d\phi C_D U^2 \approx \text{const}$$

$$\Rightarrow U \sim C_D^{-1/2}$$

$$F_{lat} \sim C_H U \Delta\theta_s \sim C_D^{1/2}$$

$$\Psi \text{ convex} \Rightarrow dC_D/dz_0 > 0$$



$$\left\{ \begin{aligned} u_*^2 &= C_D [U(z) - U_s]^2 \\ C_D &= \frac{\kappa^2}{[\Psi(z+z_0) - \Psi(z_0)]^2} \\ z_0 &= a \frac{u_*^2}{g} + b \frac{\nu}{u_*} \\ a &= \hat{a} [1 - u_w^2/u_*^2]^{-1/2} \\ u_w^2 &= g \int d\omega d\theta \gamma' N k \\ \gamma' &= \gamma'(z_0, u_*) \end{aligned} \right.$$



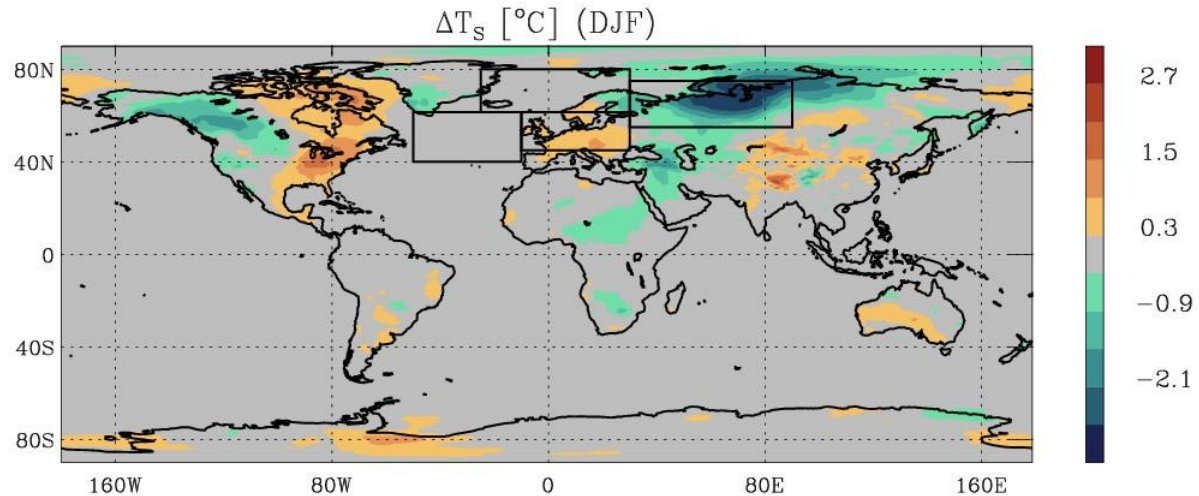
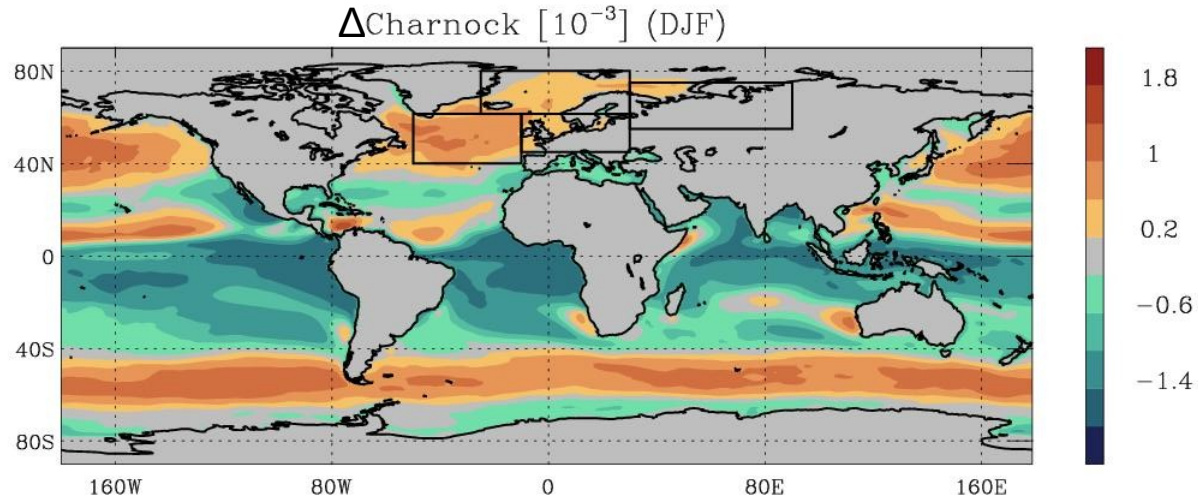
Configuration of the numerical experiments

- development version of CAM-CLUBB (based on tag cam6_3_41), FV dycore, 32 levels
- WW3 dev (tag dev/unified_0.0.2) on tn066 grid
- prescribed
 - SSTs
 - sea-ice concentration
 - atmospheric composition
- Repeating annual cycle from observed monthly climatology of the decade around year 2000
- 10 years after first year spin-up
- 6 experiments from 3 control simulations (f09, f09 de-tuned, f19)

Effect of two-way (wave-Charnock) coupling on the simulated DJF climatology

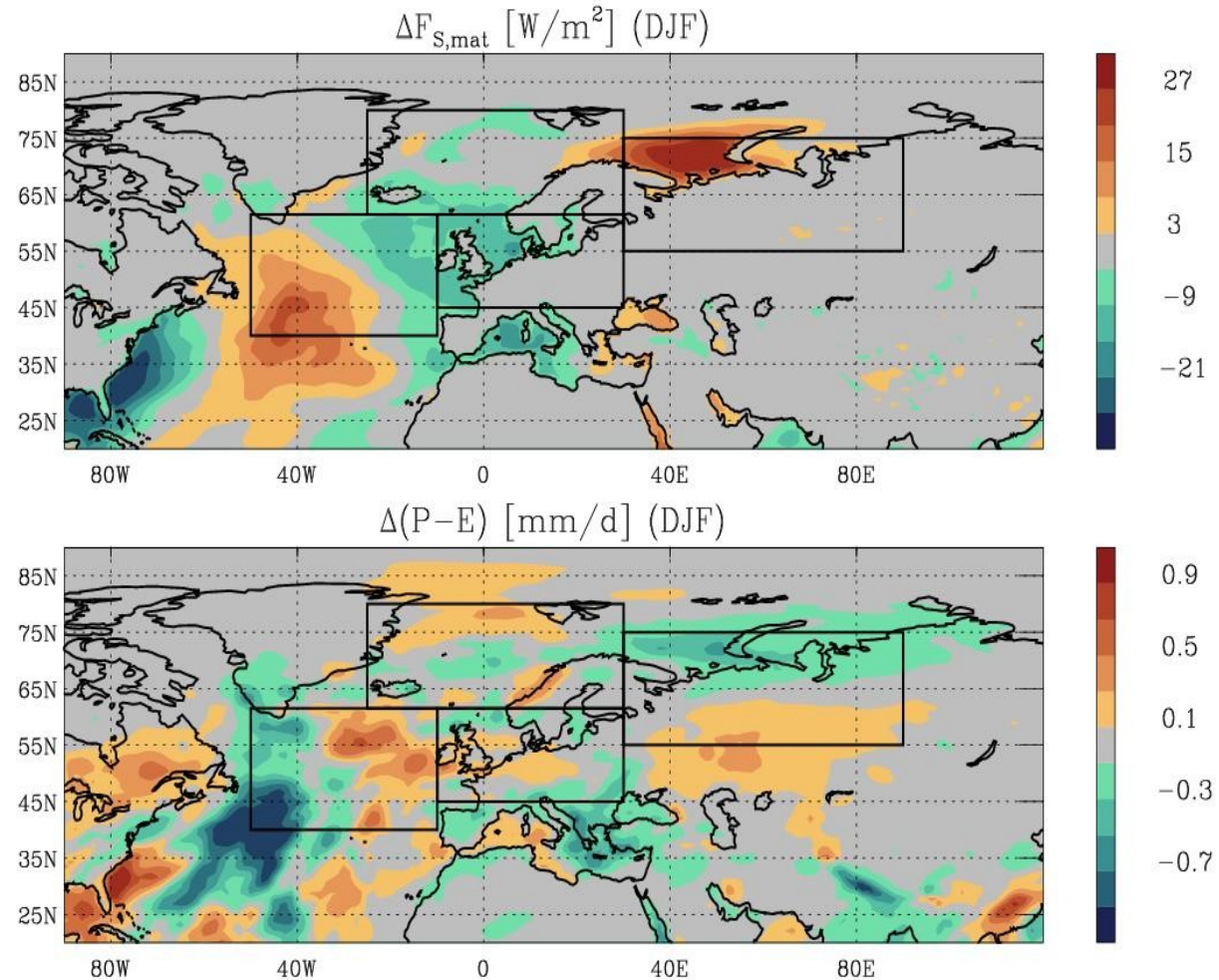
“ Δ ” = two-way minus one-way coupling

- Warmer in Europe
- Colder over Barents and Kara seas



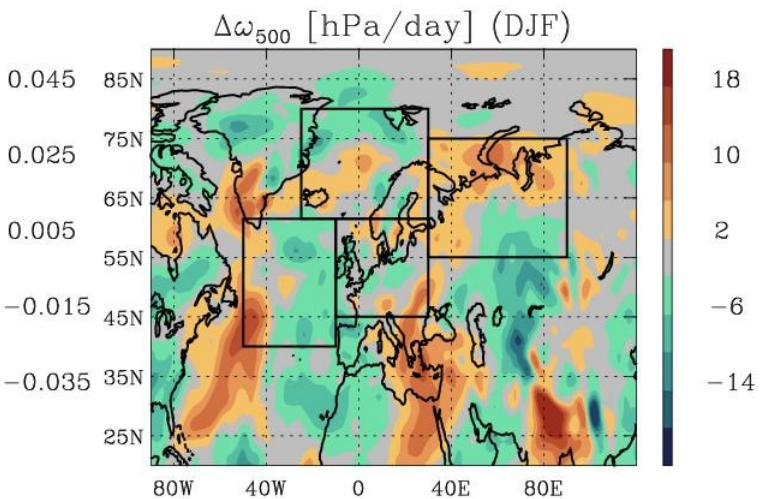
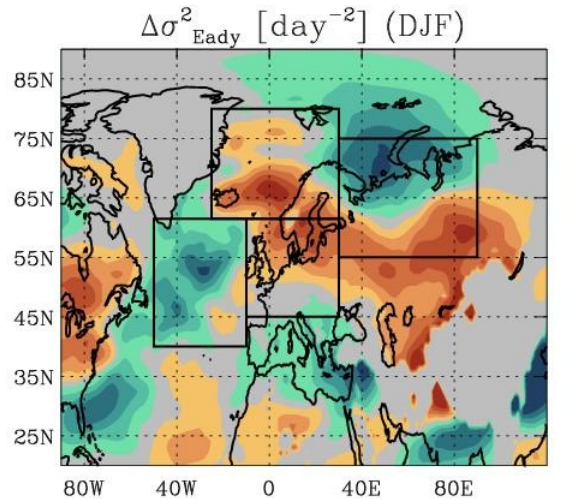
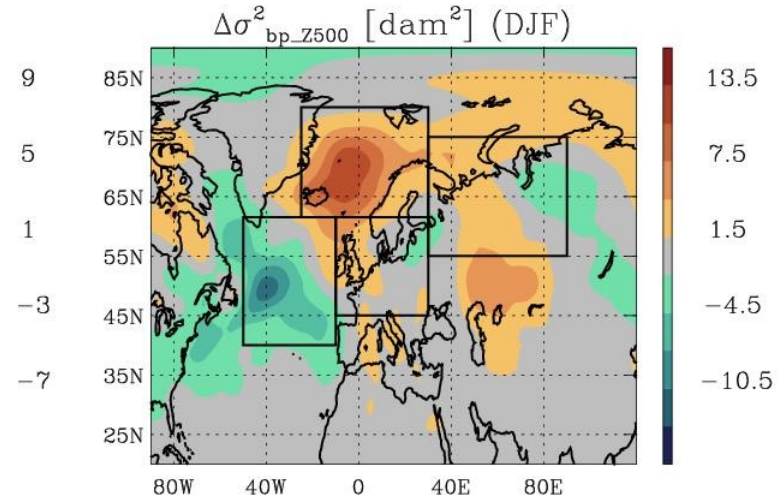
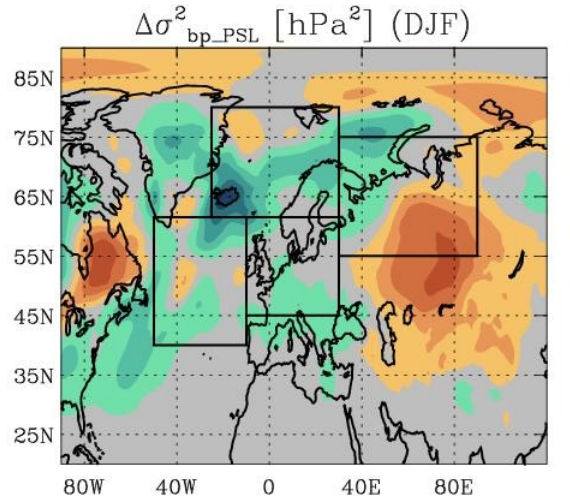
Wave-Charnock and simulated DJF climatology

- Increased evaporation over North Atlantic
- Increased precipitation downstream



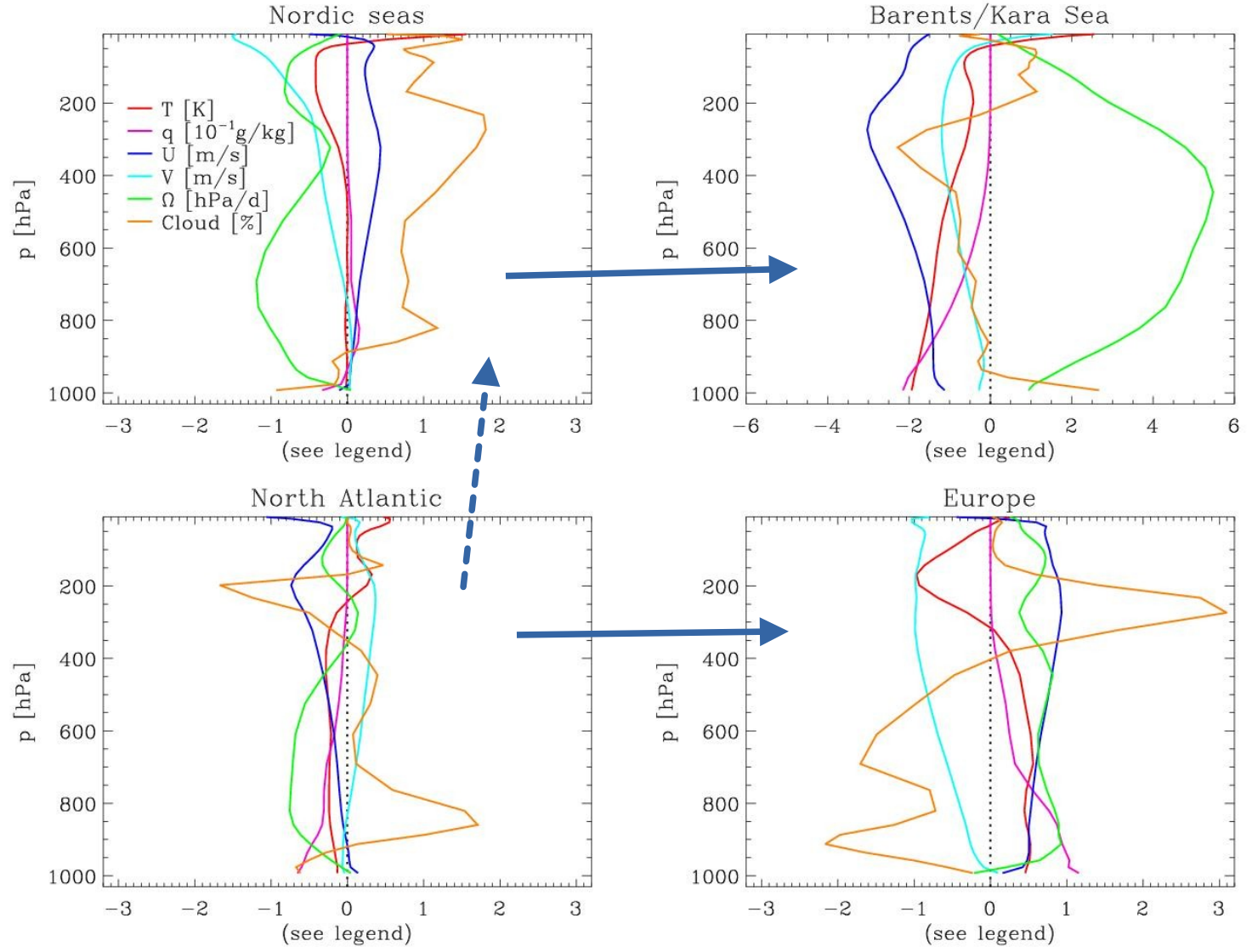
Wave-Charnock and simulated DJF climatology

- 2-6 day PSL variance decreases over ocean
- But overall baroclinic activity increases downstream of central North Atlantic
- mid-tropospheric descent over Barents and Kara seas



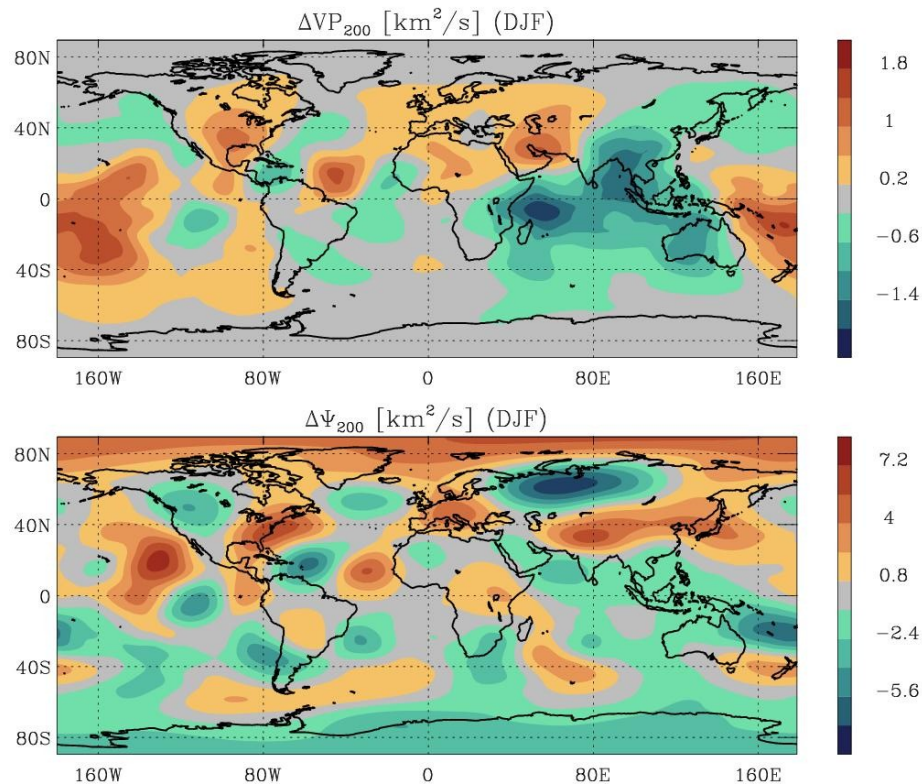
The state changes in Europe and Barents/Kara Seas consistent with downstream effects of diabatic warming over ocean

- **Westerlies and moistening over Europe**
- **Descent-drying and radiative cooling over Barents/Kara region**

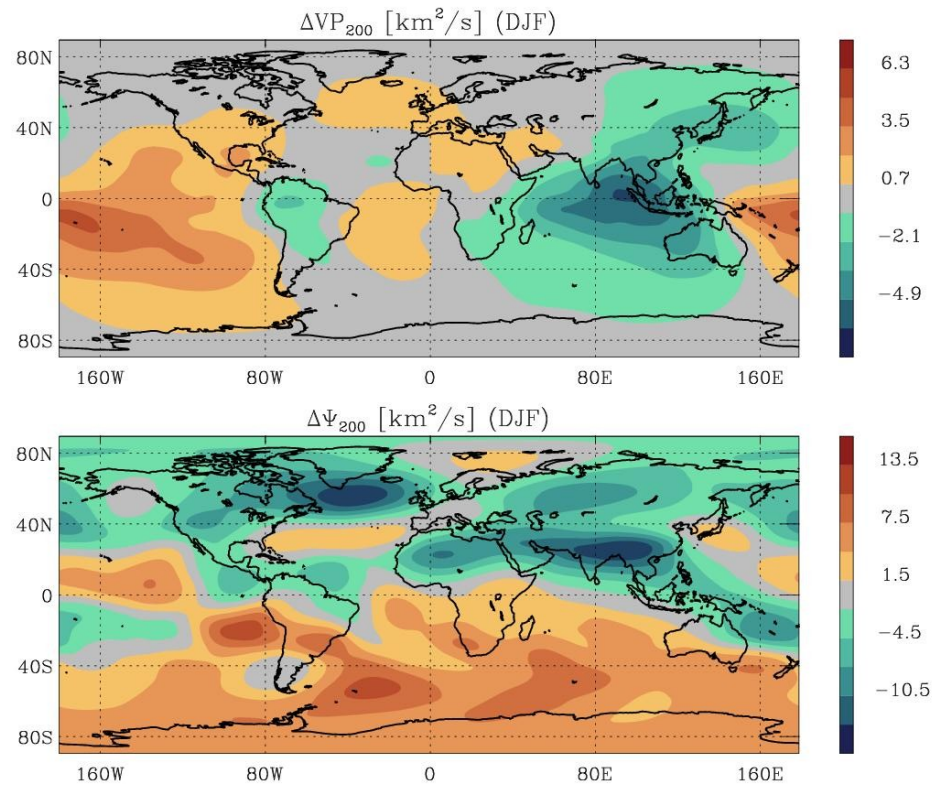


Teleconnections!

Effect of wave-Charnock

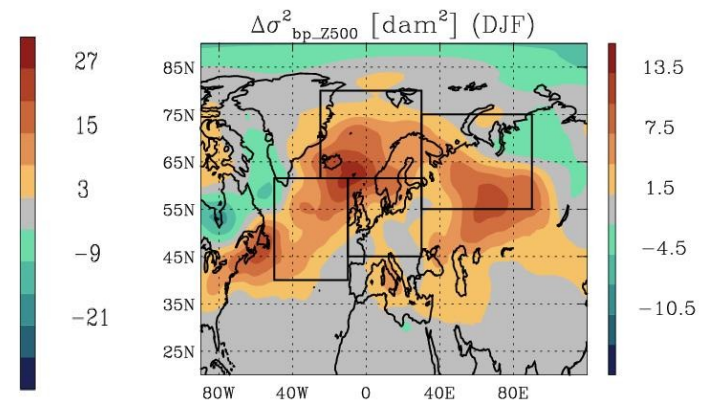
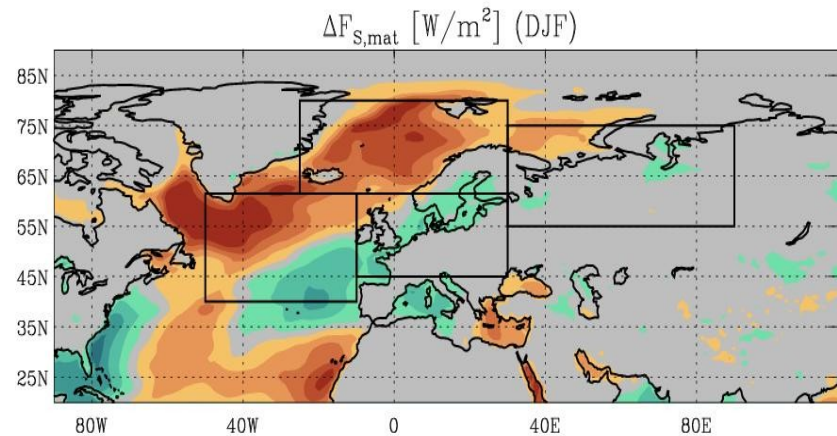
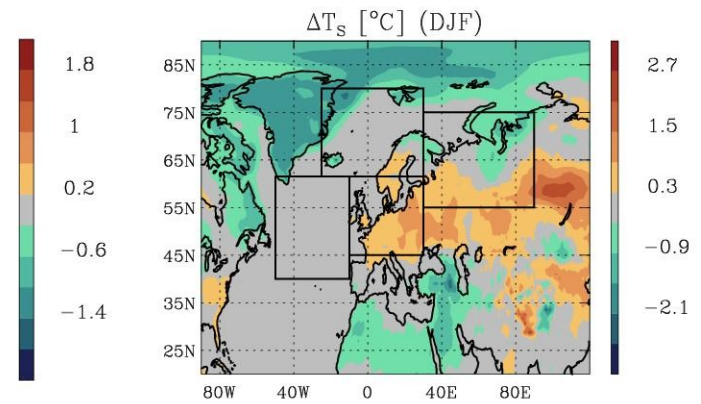
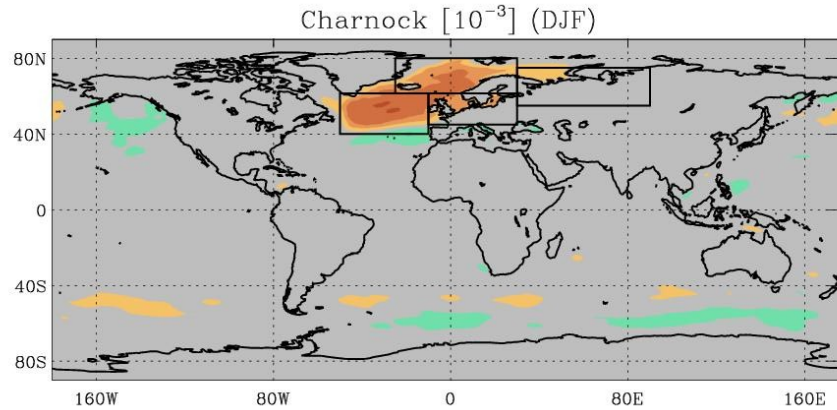


Effect of parameter (de-)tuning



Regional two-way coupling experiment (NA and Nordic Seas only)

Impacts over
the NA,
Nordic Seas
and Europe
are
qualitatively
similar, and
larger

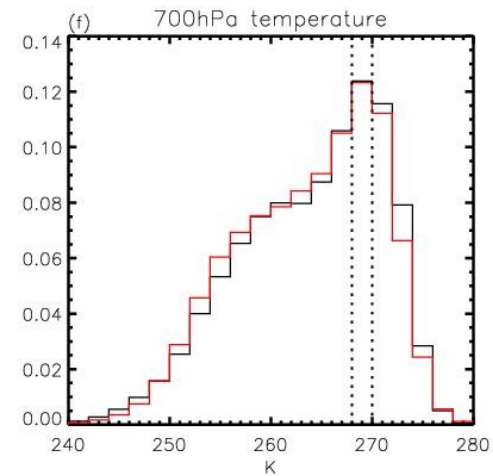
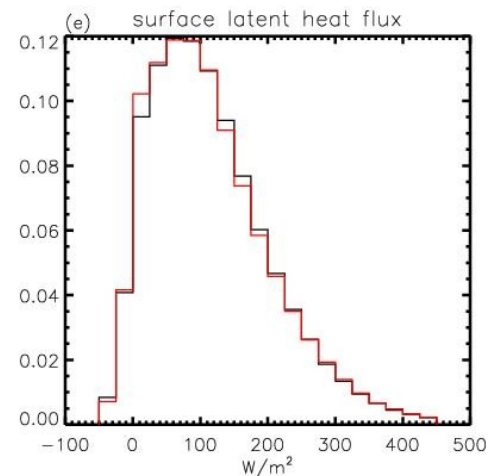
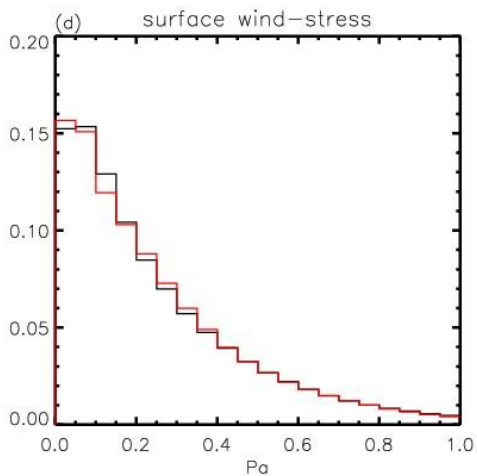
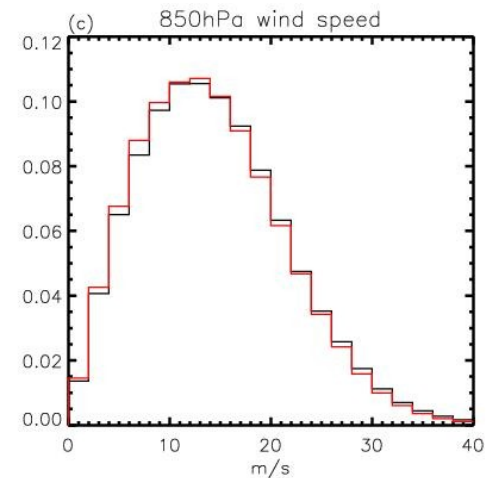
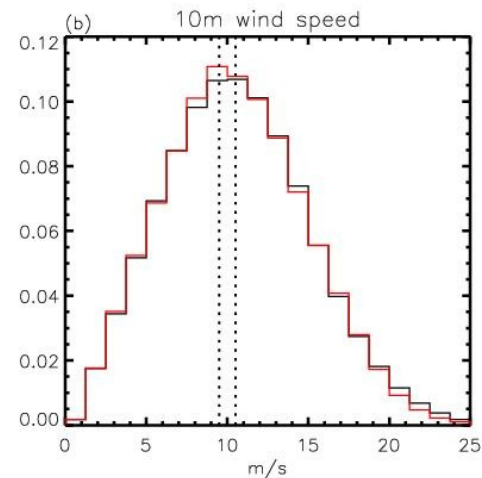
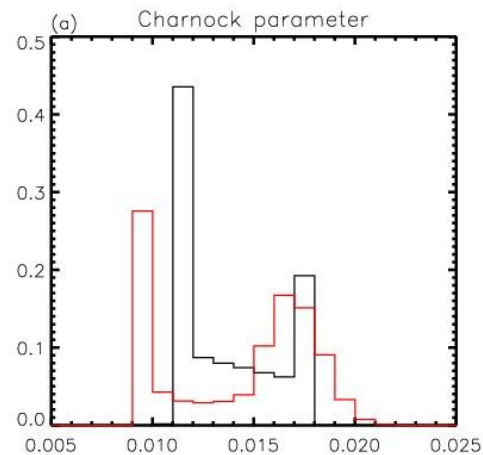


Sub-synoptic scales in the North Atlantic

— Control
— wave-Charnock

FDs of
atmospheric
PBL and
surface layer
variables.

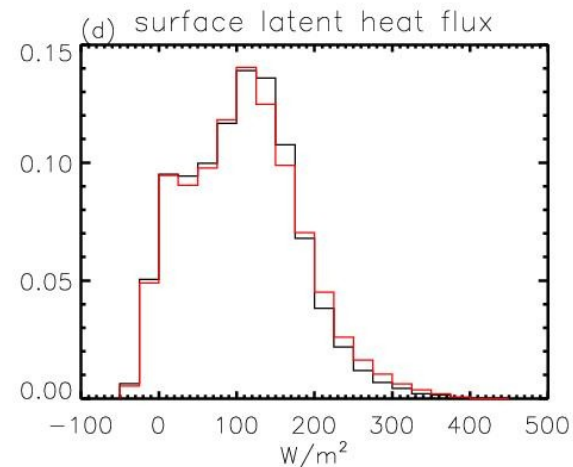
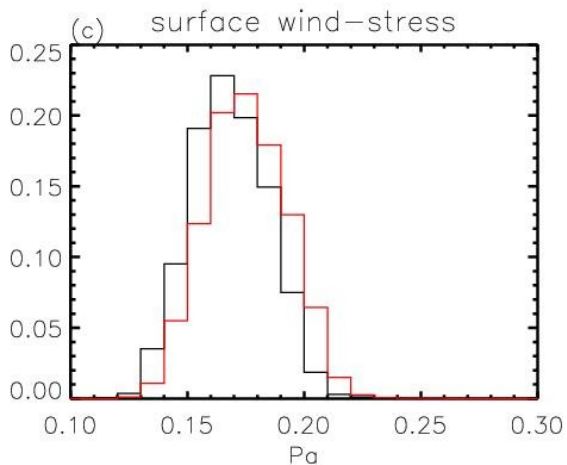
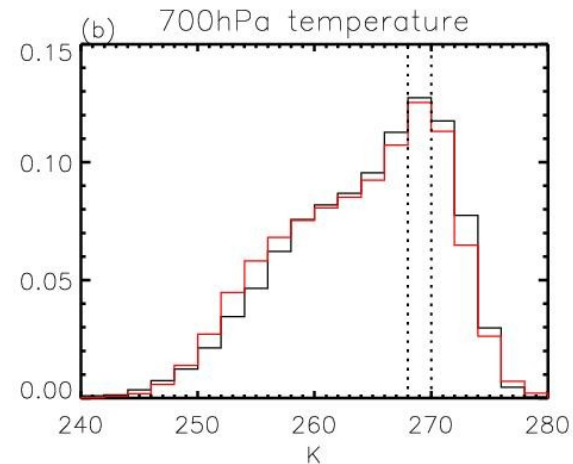
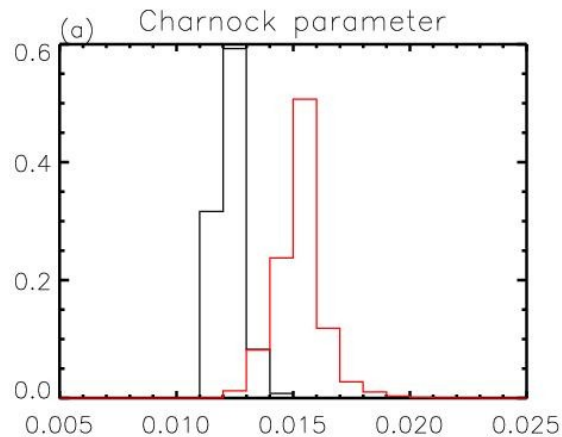
Generally
weaker
surface wind.



Sub-synoptic scales in the North Atlantic

— Control
— wave-Charnock

Under same
wind, larger wind-
stress and latent-
heat flux.



Sub-synoptic scales in the North Atlantic

— Control
— wave-Charnock

$U_{10} = 10 \text{ m/s}$
 $T_{700} = 269 \text{ K}$

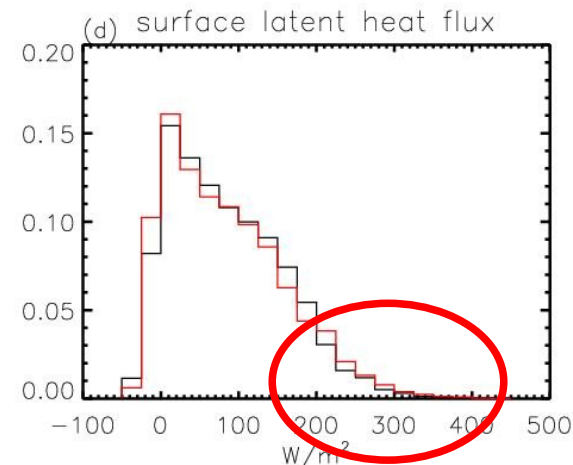
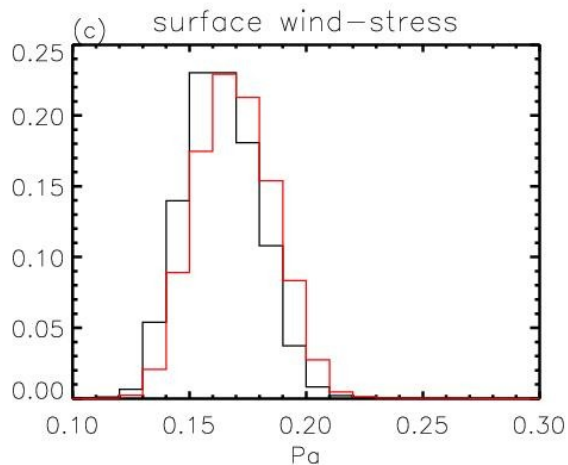
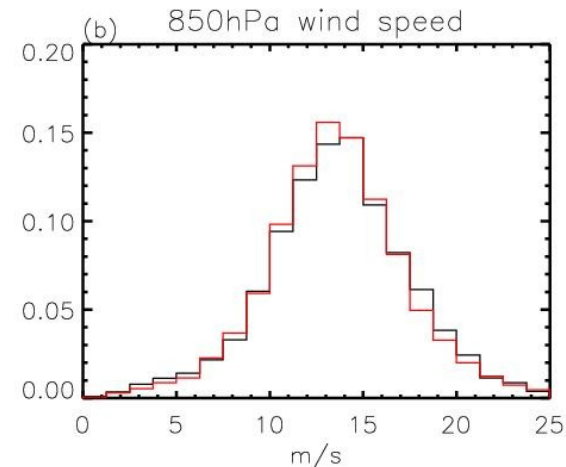
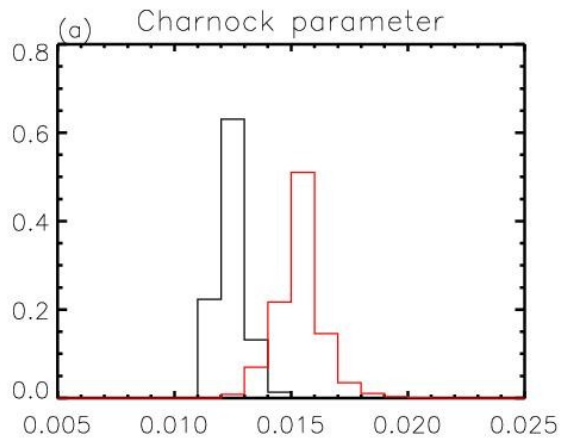
Given similar PBL conditions, wind-stress is larger and latent-heat flux still has a long “tail”.

$$\int d\phi C_D U^2 \approx \text{const}$$

$$\Rightarrow U \sim C_D^{-1/2}$$

$$F_{\text{lat}} \sim C_H U \Delta\theta_s \sim C_D^{1/2}$$

$$\Psi_{\text{convex}} \Rightarrow dC_D/dz_0 > 0$$

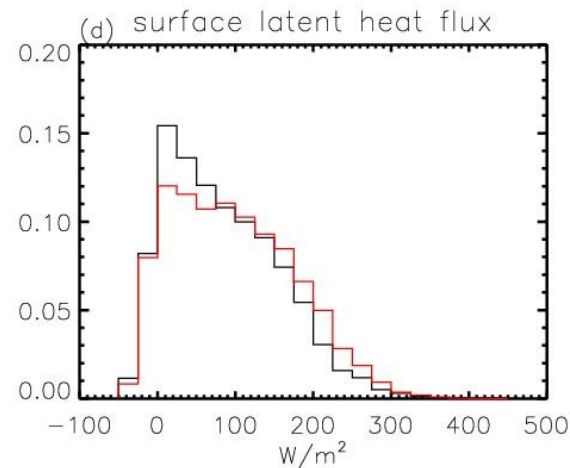
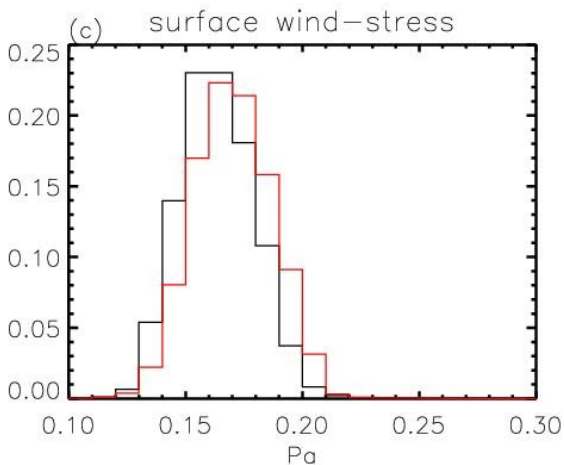
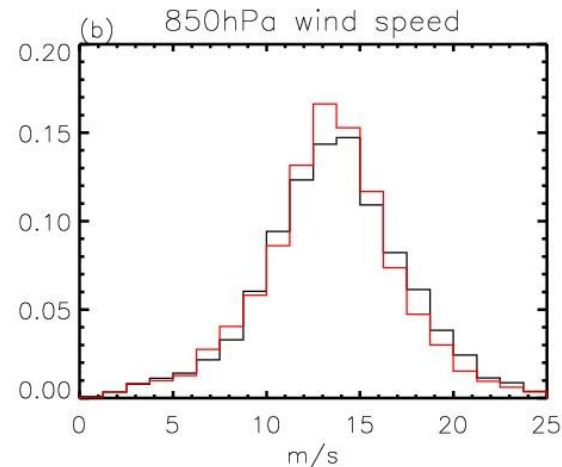
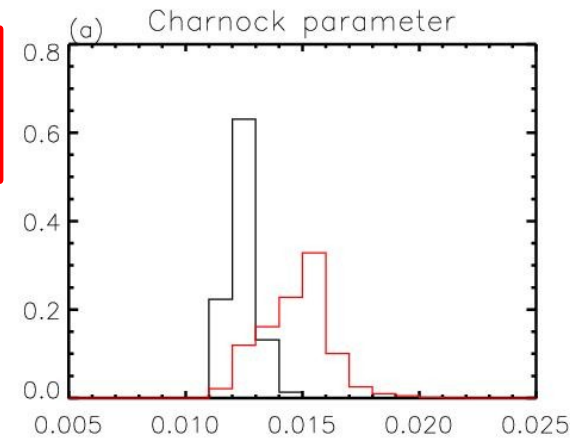


Sub-synoptic scales in the North Atlantic

— Control
— wave-Charnock

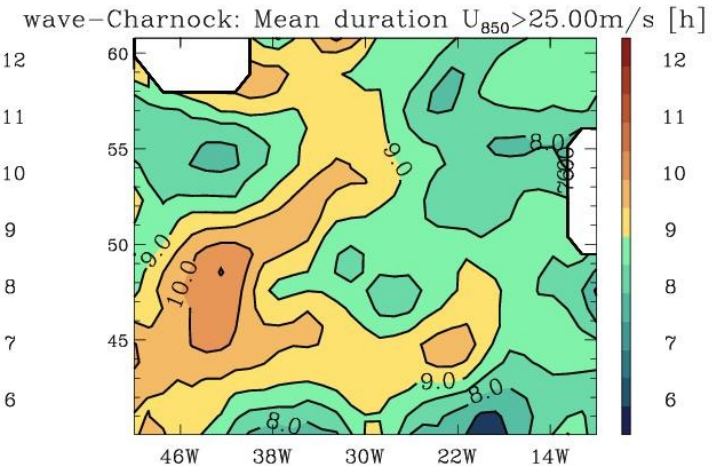
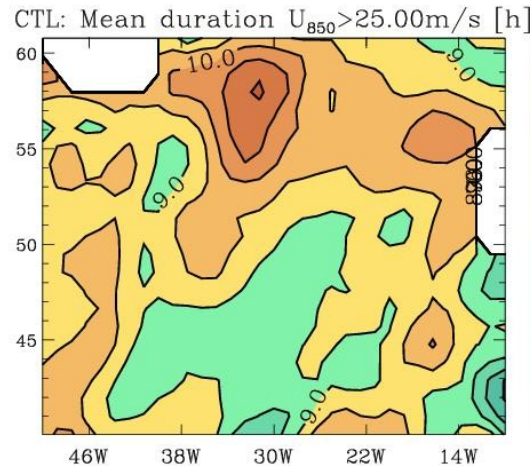
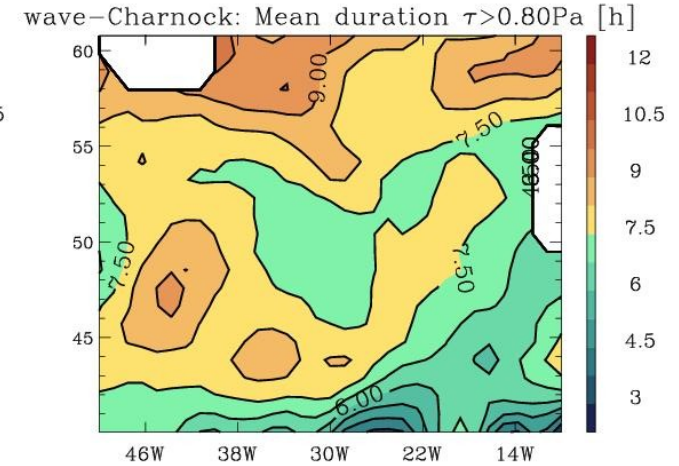
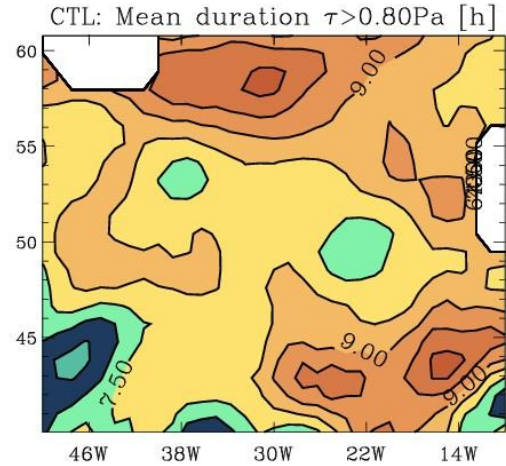
$U_{10} = 10\text{m/s}$
 $T_{700} = 269\text{K}$

The regional wave-Charnock experiment shows a much larger effect.



Sub-synoptic scales in the North Atlantic

There is some compensation between increased wind-stress and “storm” duration.



conclusions

- Two-way atmosphere-wave coupling result in robust winter warming in Europe, enhanced storminess in the Nordic Seas, and cold conditions over the Barents/Kara Seas
- These effects appear to be attributable to increased diabatic enhancement of storminess in the North Atlantic
- Downstream effect (central Asia, Siberia and Arctic) are less robust, e.g. dependent on background model climatology
- Super-imposed are tropical-mid-latitude teleconnections dependent on remote changes in wind-stress distribution, which tend to warm the Arctic; this is climate-dependent and in low-resolution simulations it can be the dominant effect